Structural Engineering and Mechanics, *Vol. 67, No. 6 (2018) 617-628*
DOI: https://doi.org/10.12989/sem.2018.67.6.617

Buckling load optimization of laminated plates resting on Pasternak foundation using TLBO

Umut Topal*[1], Trung Vo-Duy[2,3a], Tayfun Dede[4] and Ebrahim Nazarimofrad[5]

[1]*Department of Civil Engineering, Faculty of Technology, Karadeniz Technical University, Trabzon, Turkey*
[2]*Division of Computational Mathematics and Engineering, Institute for Computational Science, Ton Duc Thang University, Ho Chi Minh City, Vietnam*
[3]*Faculty of Civil Engineering Ton Duc Thang University, Ho Chi Minh City, Vietnam*
[4]*Department of Civil Engineering, Karadeniz Technical University, Trabzon, Turkey*
[5]*Department of Civil Engineering, Bu Ali Sina University, Hamedan, Iran*

(Received April 17, 2018, Revised June 25, 2018, Accepted July 3, 2018)

Abstract. This paper deals with the maximization of the critical buckling load of simply supported antisymmetric angle-ply plates resting on Pasternak foundation subjected to compressive loads using teaching learning based optimization method (TLBO). The first order shear deformation theory is used to obtain governing equations of the laminated plate. In the present optimization problem, the objective function is to maximize the buckling load factor and the design variables are the fibre orientation angles in the layers. Computer programming is developed in the MATLAB environment to estimate optimum stacking sequences of laminated plates. A comparison also has been performed between the TLBO, genetic algorithm (GA) and differential evolution algorithm (DE). Some examples are solved to show the applicability and usefulness of the TLBO for maximizing the buckling load of the plate via finding optimum stacking sequences of the plate. Additionally, the influences of different number of layers, plate aspect ratios, foundation parameters and load ratios on the optimal solutions are investigated.

Keywords: laminated composite plates; Pasternak foundation; optimization; TLBO; buckling

1. Introduction

The buckling problem of the rectangular plates subjected to external loads, resting on an elastic foundation, is widely used in a variety of engineering structures, such as civil engineering, aerospace, biomechanics, petrochemical, and marine industries, as well as mechanical, nuclear, and electrical applications. Rectangular plates resting on an elastic foundation are frequently used as structural elements in modeling of the engineering problems, such as concrete roads, mat foundations of buildings, and reinforced concrete pavements of the airport runways.

There have been a considerable number of studies on the buckling load optimization of laminated composite structures. Topal (2017) investigated buckling load optimization of symmetric angle-ply laminated stepped flat columns under axial compression load. The modified feasible direction method was used for the optimization algorithm. Topal and Ozturk (2014) used artificial bee colony algorithm to optimize the stacking sequences of the simply supported antisymmetric laminated composite plates with the critical buckling load. Nicholas *et al.* (2014) investigated buckling load optimization of the composite plate with cutout using a genetic algorithm based optimization technique. Ehsani and Rezaeepazhand (2016) optimized the stacking sequence and pattern composition of the laminated grid plates subjected to uniaxial or shear buckling load using genetic algorithm. Henrichsen *et al.* (2015) conducted robust buckling optimal design of laminated composite structures. Huu *et al.* (2016) proposed a novel numerical optimization procedure with mixed integer and continuous design variables for optimal design of laminated composite plates subjected to buckling loads. Vosoughi *et al.* (2017) studied buckling load optimization of stiffened laminated composite plate using finite element, genetic algorithm and particle swarm optimization methods. Jing *et al.* (2015) maximized the buckling load of composite laminates using permutation search algorithm. Karakaya and Soykasap (2009) used genetic algorithm and generalized pattern search algorithm for optimal stacking sequence of a composite panel subject to biaxial in-plane compressive loads. Deveci *et al.* (2016) proposed an optimization procedure to find the optimum stacking sequence designs of laminated composite plates in different fiber angle domains for maximum buckling resistance. Adali *et al.* (2003) presented optimal designs of symmetrically laminated composite plates subjected to a biaxial uncertain buckling load using anti-optimization. Narita and Turvey (2004) maximized the buckling loads of symmetrically laminated composite rectangular plates using a layerwise optimization approach. Hajmohammad *et al.* (2013) investigated buckling load optimization of composite laminates using neural network and genetic algorithm. Aymerich and Serra (2008) optimized buckling

*Corresponding author, Professor
E-mail: utopal@ktu.edu.tr
[a]Ph.D.
E-mail: voduytrung@tdt.edu.vn

http://www.techno-press.com/journals/sem&subpage=7
ISSN: 1225-4568 (Print), 1598-6217 (Online)

load of laminates using ant colony optimization algorithm. Sebaey *et al.* (2011) maximized the buckling load of laminated composite panels using ant colony algorithm. Soremekun *et al.* (2001) explored the several generalized elitist procedures for the design of composite laminates. Kaveh *et al.* (2018) presented the application of the biogeography-based optimization and some of its variants in the optimization of stacking sequence of laminated composites. Erdal and Sonmez (2005) presented a method to find globally optimum designs for two-dimensional composite structures subject to given in-plane static loads for which the critical failure mode is buckling. Almeida (2016) investigated the application of the harmony search algorithm and some of its variants in the optimization of the stacking sequence of laminated composites. Vosoughi *et al.* (2017) obtained optimum stacking sequences of thick laminated composite plate to maximize its buckling load via employing the finite element, genetic algorithms and particle swarm optimization methods.

On the other hand, buckling load optimization of laminated composite plates resting on the elastic foundation has not yet been thoroughly investigated. Therefore, this paper focuses on the maximization of the critical buckling load of simply supported antisymmetric angle-ply plates resting on Pasternak foundation subjected to compressive loads using teaching learning based optimization method (TLBO). The first order shear deformation theory is used to obtain governing equations of the laminated plate. In the present optimization problem, the objective function is to maximize the buckling load factor and the design variables are the fibre orientation angles in the layers. Computer programming is developed in the MATLAB environment to estimate optimum stacking sequences of laminated plates. A comparison also has been performed between the TLBO, genetic algorithm (GA) and differential evolution algorithm (DE). Some examples are solved to show applicability and usefulness of the TLBO for maximizing the buckling load of the plate via finding optimum stacking sequences of the plate. Additionally, the influences of different number of layers, plate aspect ratios, foundation parameters and load ratios on the optimal solutions are investigated.

2. Basic equations

Consider a rectangular laminated composite plate with constant thickness of *h* and in-plane dimensions of *a* and *b* resting on Pasternak foundation as shown in Fig. 1.

For a flat moderately thick laminated plate, based on the first order shear deformation theory, the displacement field is defined as

$$\mathbf{u}(x,y,z) = u_o(x,y) + \psi_x(x,y)$$
$$\mathbf{v}(x,y,z) = v_o(x,y) + \psi_y(x,y) \quad (1)$$
$$\mathbf{w}(x,y,z) = w_o(x,y)$$

where u_o, v_o and w_o denote the translation displacements along x, y and z directions of a point at the mid-plane, respectively; ψ_x and ψ_y represent rotations of a transverse normal about y and x axes, respectively. The

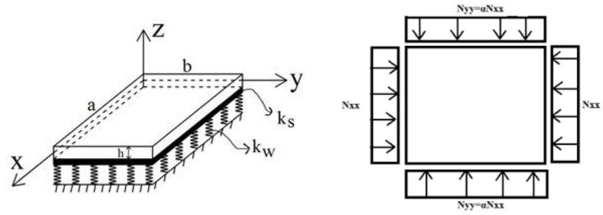

Fig. 1 Geometry and load conditions of a laminated composite plate resting on Pasternak foundation

displacement-strain relations, taking Eq. (1) account are

$$\boldsymbol{\varepsilon} = \begin{Bmatrix} \varepsilon_p \\ \gamma_s \end{Bmatrix} + \begin{Bmatrix} z\varepsilon_b \\ 0 \end{Bmatrix} \quad (2)$$

where the following definitions apply

$$\boldsymbol{\varepsilon_p} = \begin{Bmatrix} u_{o,x} \\ v_{o,y} \\ u_{o,y} + v_{o,x} \end{Bmatrix}, \quad \boldsymbol{\varepsilon_b} = \begin{Bmatrix} \psi_{x,x} \\ \psi_{y,y} \\ \psi_{x,y} + \psi_{y,x} \end{Bmatrix},$$
$$\boldsymbol{\gamma_s} = \begin{Bmatrix} w_{o,x} + \psi_x \\ w_{o,y} + \psi_y \end{Bmatrix} \quad (3)$$

Following the linear stress-strain displacement relations, the constitutive law of the plate may be expressed as

$$\boldsymbol{\sigma} = D_m(\varepsilon_p + z\varepsilon_b), \boldsymbol{\tau} = D_s\gamma_s \quad (4)$$

where the following definitions apply

$$\boldsymbol{\sigma} = \begin{Bmatrix} \sigma_x \\ \sigma_y \\ \sigma_{xy} \end{Bmatrix}, \quad \boldsymbol{\tau} = \begin{Bmatrix} \tau_{xz} \\ \tau_{yz} \end{Bmatrix}, \mathbf{D_m} = \begin{bmatrix} \overline{Q}_{11} & \overline{Q}_{12} & \overline{Q}_{16} \\ \overline{Q}_{12} & \overline{Q}_{22} & \overline{Q}_{26} \\ \overline{Q}_{16} & \overline{Q}_{26} & \overline{Q}_{66} \end{bmatrix},$$
$$\mathbf{D_S} = \begin{bmatrix} \overline{Q}_{44} & \overline{Q}_{45} \\ \overline{Q}_{45} & \overline{Q}_{55} \end{bmatrix} \quad (5)$$

where as known from the transformation rule is fiber reinforced composite materials, $\overline{Q}_{ij}$ is the transformed reduced stiffness matrix and can be written as

$$\begin{bmatrix} \overline{\mathbf{Q}}_{\mathbf{11}} \\ \overline{\mathbf{Q}}_{\mathbf{12}} \\ \overline{\mathbf{Q}}_{\mathbf{22}} \\ \overline{\mathbf{Q}}_{\mathbf{16}} \\ \overline{\mathbf{Q}}_{\mathbf{26}} \\ \overline{\mathbf{Q}}_{\mathbf{66}} \end{bmatrix} = \begin{bmatrix} c^4 & 2c^2s^2 & s^4 & 4c^2s^2 \\ c^2s^2 & c^4+s^4 & c^2s^2 & -4c^2s^2 \\ s^4 & 2c^2s^2 & c^4 & 4c^2s^2 \\ c^3s & cs^3-c^3s & -cs^3 & -2c^3s+2cs^3 \\ cs^3 & c^3s-cs^3 & -c^3s & 2c^3s-2cs^3 \\ c^2s^2 & -2c^2s^2 & c^2s^2 & (c^2-s^2)^2 \end{bmatrix} \begin{bmatrix} Q_{11} \\ Q_{12} \\ Q_{22} \\ Q_{26} \end{bmatrix} \quad (6)$$

$$\begin{bmatrix} \overline{\mathbf{Q}}_{\mathbf{44}} \\ \overline{\mathbf{Q}}_{\mathbf{45}} \\ \overline{\mathbf{Q}}_{\mathbf{55}} \end{bmatrix} = \begin{bmatrix} c^2 & s^2 \\ -cs & cs \\ s^2 & c^2 \end{bmatrix} \begin{bmatrix} Q_{44} \\ Q_{55} \end{bmatrix}$$

where in the above equation, Q_{ij} is the elastic coefficients in the material coordinate, $c = \cos\theta$ and $s = \sin\theta$. Also θ is the angle of the lamination against the plate x-axis.

The membrane force vector N, bending moment vector M and transverse shear force vector Q can be obtained as follows

$$\mathbf{N} = A_m \varepsilon_p + B\varepsilon_b, \mathbf{M} = B\varepsilon_p + D\varepsilon_b, \mathbf{Q} = A_s \gamma_s \tag{7}$$

where the stiffness matrices of the laminated composite plate are obtained as

$$(\mathbf{A_m}, \mathbf{B}, \mathbf{D}, \mathbf{A_s}) = \sum_{k=1}^{N_L} \int_{h_{k-1}}^{h_k} (D_m, zD_m, z^2 D_m, KD_s) dz \tag{8}$$

and K denotes the transverse shear correction coefficient, which is suggested as K=5/6. The governing differential equations of the plate can be given as below

$$\begin{aligned}
&\frac{\partial N_{xx}}{\partial x} + \frac{\partial N_{xy}}{\partial y} = 0 \\
&\frac{\partial N_{xy}}{\partial x} + \frac{\partial N_{yy}}{\partial y} = 0 \\
&\frac{\partial Q_x}{\partial x} + \frac{\partial Q_y}{\partial y} + \widehat{N}_{xx} \frac{\partial^2 w_0}{\partial x^2} + \widehat{N}_{yy} \frac{\partial^2 w_0}{\partial y^2} + 2\widehat{N}_{xy} \frac{\partial^2 w_0}{\partial x \partial y} - k_w w_o + k_s\left(\frac{\partial^2 w_0}{\partial x^2} + \frac{\partial^2 w_0}{\partial y^2}\right) = 0 \\
&\frac{\partial M_{xx}}{\partial x} + \frac{\partial M_{xy}}{\partial y} - Q_x = 0 \\
&\frac{\partial M_{xy}}{\partial x} + \frac{\partial M_{yy}}{\partial y} - Q_y = 0
\end{aligned} \tag{9}$$

where k_w are k_s are the Winkler foundation stiffness and the shear stiffness of the elastic foundation, respectively. Note that if k_s=0 Pasternak model reduces to the Winkler foundation model. By putting Eq. (7) to Eq. (9), Eq. (9) can be written as

$$\begin{aligned}
&\frac{\partial}{\partial x}\left[A_{11}\frac{\partial u_0}{\partial x} + A_{12}\frac{\partial v_0}{\partial y} + A_{16}\left(\frac{\partial u_0}{\partial y} + \frac{\partial v_0}{\partial x}\right) + B_{11}\frac{\partial \psi_x}{\partial x} + B_{12}\frac{\partial \psi_y}{\partial y} + B_{16}\left(\frac{\partial \psi_x}{\partial y} + \frac{\partial \psi_y}{\partial x}\right)\right] \\
&+ \frac{\partial}{\partial y}\left[A_{16}\frac{\partial u_0}{\partial x} + A_{26}\frac{\partial v_0}{\partial y} + A_{66}\left(\frac{\partial u_0}{\partial y} + \frac{\partial v_0}{\partial x}\right) + B_{16}\frac{\partial \psi_x}{\partial x} + B_{26}\frac{\partial \psi_y}{\partial y} + B_{66}\left(\frac{\partial \psi_x}{\partial y} + \frac{\partial \psi_y}{\partial x}\right)\right] = 0 \\
&\frac{\partial}{\partial x}\left[A_{16}\frac{\partial u_0}{\partial x} + A_{26}\frac{\partial v_0}{\partial y} + A_{66}\left(\frac{\partial u_0}{\partial y} + \frac{\partial v_0}{\partial x}\right) + B_{16}\frac{\partial \psi_x}{\partial x} + B_{26}\frac{\partial \psi_y}{\partial y} + B_{66}\left(\frac{\partial \psi_x}{\partial y} + \frac{\partial \psi_y}{\partial x}\right)\right] \\
&+ \frac{\partial}{\partial y}\left[A_{12}\frac{\partial u_0}{\partial x} + A_{22}\frac{\partial v_0}{\partial y} + A_{26}\left(\frac{\partial u_0}{\partial y} + \frac{\partial v_0}{\partial x}\right) + B_{12}\frac{\partial \psi_x}{\partial x} + B_{22}\frac{\partial \psi_y}{\partial y} + B_{26}\left(\frac{\partial \psi_x}{\partial y} + \frac{\partial \psi_y}{\partial x}\right)\right] = 0 \\
&\frac{\partial}{\partial x}\left[KA_{45}\left(\frac{\partial w_0}{\partial y} + \psi_y\right) + KA_{55}\left(\frac{\partial w_0}{\partial x} + \psi_x\right)\right] + \frac{\partial}{\partial y}\left[KA_{44}\left(\frac{\partial w_0}{\partial y} + \psi_y\right) + KA_{45}\left(\frac{\partial w_0}{\partial x} + \psi_x\right)\right] + \widehat{N}_{xx}\frac{\partial^2 w_0}{\partial x^2} \\
&+ \widehat{N}_{yy}\frac{\partial^2 w_0}{\partial y^2} + 2\widehat{N}_{xy}\frac{\partial^2 w_0}{\partial x \partial y} - k_w w_o + k_s\left(\frac{\partial^2 w_0}{\partial x^2} + \frac{\partial^2 w_0}{\partial y^2}\right) = 0 \\
&\frac{\partial}{\partial x}\left[B_{11}\frac{\partial u_0}{\partial x} + B_{12}\frac{\partial v_0}{\partial y} + B_{16}\left(\frac{\partial u_0}{\partial y} + \frac{\partial v_0}{\partial x}\right) + D_{11}\frac{\partial \psi_x}{\partial x} + D_{12}\frac{\partial \psi_y}{\partial y} + D_{16}\left(\frac{\partial \psi_x}{\partial y} + \frac{\partial \psi_y}{\partial x}\right)\right] \\
&+ \frac{\partial}{\partial y}\left[B_{16}\frac{\partial u_0}{\partial x} + B_{26}\frac{\partial v_0}{\partial y} + B_{66}\left(\frac{\partial u_0}{\partial y} + \frac{\partial v_0}{\partial x}\right) + D_{16}\frac{\partial \psi_x}{\partial x} + D_{26}\frac{\partial \psi_y}{\partial y} + D_{66}\left(\frac{\partial \psi_x}{\partial y} + \frac{\partial \psi_y}{\partial x}\right)\right] \\
&- \left[KA_{45}\left(\frac{\partial w_0}{\partial y} + \psi_y\right) + KA_{55}\left(\frac{\partial w_0}{\partial x} + \psi_x\right)\right] = 0 \\
&\frac{\partial}{\partial x}\left[B_{16}\frac{\partial u_0}{\partial x} + B_{26}\frac{\partial v_0}{\partial y} + B_{66}\left(\frac{\partial u_0}{\partial y} + \frac{\partial v_0}{\partial x}\right) + D_{16}\frac{\partial \psi_x}{\partial x} + D_{26}\frac{\partial \psi_y}{\partial y} + D_{66}\left(\frac{\partial \psi_x}{\partial y} + \frac{\partial \psi_y}{\partial x}\right)\right] \\
&+ \frac{\partial}{\partial y}\left[B_{12}\frac{\partial u_0}{\partial x} + B_{22}\frac{\partial v_0}{\partial y} + B_{26}\left(\frac{\partial u_0}{\partial y} + \frac{\partial v_0}{\partial x}\right) + D_{12}\frac{\partial \psi_x}{\partial x} + D_{22}\frac{\partial \psi_y}{\partial y} + D_{26}\left(\frac{\partial \psi_x}{\partial y} + \frac{\partial \psi_y}{\partial x}\right)\right] \\
&- \left[KA_{44}\left(\frac{\partial w_0}{\partial y} + \psi_y\right) + KA_{45}\left(\frac{\partial w_0}{\partial x} + \psi_x\right)\right] = 0
\end{aligned} \tag{10}$$

In this study, the buckling load of the simply supported antisymmetric angle-ply laminated composite plate is analyzed by using a Navier-type solution. The simply supported condition is given as (Reddy 2004)

$$\begin{aligned}
&u_0(0,y) = 0, \quad u_0(a,y) = 0, \quad v_0(x,0) = 0, \quad u_0(x,b) = 0, \\
&w_0(x,0) = 0, \quad w_0(x,b) = 0, \quad w_0(0,y) = 0, \quad w_0(a,y) = 0, \\
&\psi_x(x,0) = 0, \quad \psi_x(x,b) = 0, \quad \psi_y(0,y) = 0, \quad \psi_y(a,y) = 0,
\end{aligned} \tag{11}$$

$$N_{xy}(x,0)=0,\quad N_{xy}(x,b)=0,\quad N_{xy}(0,y)=0,\quad N_{xy}(a,y)=0,$$

$$M_{yy}(x,0)=0,\quad M_{yy}(x,b)=0,\quad M_{xx}(0,y)=0,\quad M_{xx}(a,y)=0$$

The displacement formula which satisfies these boundary conditions is assumed to be

$$\begin{aligned}
\mathbf{u_0}(x,y) &= \sum_{n=1}^{\infty}\sum_{m=1}^{\infty} U_{mn}\sin\alpha x\ \cos\beta y \\
\mathbf{v_0}(x,y) &= \sum_{n=1}^{\infty}\sum_{m=1}^{\infty} V_{mn}\cos\alpha x\ \sin\beta y \\
\mathbf{w_0}(x,y) &= \sum_{n=1}^{\infty}\sum_{m=1}^{\infty} W_{mn}\sin\alpha x\ \sin\beta y \\
\boldsymbol{\psi_x}(x,y) &= \sum_{n=1}^{\infty}\sum_{m=1}^{\infty} X_{mn}\cos\alpha x\ \sin\beta y \\
\boldsymbol{\psi_y}(x,y) &= \sum_{n=1}^{\infty}\sum_{m=1}^{\infty} Y_{mn}\sin\alpha x\ \cos\beta y
\end{aligned} \tag{12}$$

where U_{mn}, V_{mn}, W_{mn}, X_{mn}, Y_{mn} are the arbitrary coefficients, $\alpha = m\pi/a$ and $\alpha = n\pi/b$. For the buckling analysis, the formulation of a laminated composite plate can be obtained as follows

$$\left(\mathbf{K_L} + \boldsymbol{\lambda_{cr}}\mathbf{K_g}\right)\delta = 0 \tag{13}$$

where in the above equation, K_L and K_g are the linear stiffness matrix and geometric stiffness matrix, respectively, λ_{cr} is the critical buckling load and δ is the displacement vector. Eq. (13) is an eigenvalue problem. For a nontrivial solution, the determinant of the coefficient matrix should be zero. The roots of the determinants are the buckling loads. The lowest one is called critical buckling load.

3. Optimization algorithms

Optimal design of the structures is one of the most active fields of structural engineering. Different optimization approaches can be employed to optimize the structural performance of the laminated composites against buckling load due to design variables such as the fiber orientations and stacking sequence. Metaheuristics are the suitable tools for the global search of large and complex problems with affordable computational time and accuracy that are usually inspired by the nature (Kaveh 2017, Kaveh and Khayatazad 2012, Kaveh and Farhoudi 2013, Kaveh and Mahdavi 2014, Kaveh and Ghazaan 2017, Moez *et al.* 2016). In this study, TLBO, GA and DE algorithms are used for buckling load optimization of antisymmetric angle-ply laminated composite plates.

3.1 Teaching-learning based optimization (TLBO)

Teaching-learning is an important process where every individual tries to learn something from other individuals to improve themselves. Rao *et al.* (2011) proposed an algorithm, known as Teaching-Learning-Based Optimization (TLBO), which simulates the traditional teaching-learning phenomenon of a classroom. In the literature, there are some optimization researches using TLBO algorithm (Daloglu 2018, Artar *et al.* 2017, Artar 2016). The algorithm simulates two fundamental modes of learning: (i) teacher phase and (ii) learner phase. TLBO is a population based algorithm, where a group of students (i.e., learner) is considered the population and the different subjects offered to the learners are analogous with the different design variables of the optimization problem. The results of the learner are analogous to the fitness value of the optimization problem. The best solution in the entire population is considered as the teacher. The operation of the TLBO algorithm is explained below with teacher phase and learner phase.

3.1.1 Teaching phase

This phase of the algorithm simulates the learning of the students (i.e., learners) through the teacher. During this phase, a teacher conveys knowledge among the learners and makes an effort to increase the mean result of the class. A student within the population consists of a number of design variables (X_i) of the problem. In this study, the design variables are the fibre orientations (θ_i) of the layers.

$$Xstudent_i = \left[X_{i,1}\ X_{i,2}\ \dots\ X_{i,D_n}\right],\quad i = 1, 2, \dots, P_n \tag{14}$$

where, D_n is number of design variables, P_n is size of population. Teacher phase is formulated as follows

$$student_{new\_i} = student_i + r*(teacher - TF*mean) \tag{15}$$

where $X\,student_{new\_i}$ and $X\,student_i$ are the new and old positions of the ith learner, $X\,teacher$ is the position of the current teacher, r is the random number within the range [0,1]. All learners should be re-evaluated after each iteration of the teacher phase. If $X\,student_{new\_i}$ is better than $X\,student_i$, $X\,student_{new\_i}$ will be accepted and flowed to Learner phase, otherwise $X\,student_i$ is not changed. TF is the teaching factor, and its value is heuristically set to either 1 or 2. It is determined using Eq. (16).

$$TF = round[1 + rand(0,1)\{2\ \ 1\}] \tag{16}$$

The mean parameter $Xmean$ of each subject of the learners in the class at generation is given as

$$Xmean = \left[Xmean(X_1), Xmean(X_2), \dots\dots, Xmean\left(X_{D_n}\right)\right] \tag{17}$$

3.1.2 Learning phase

This phase of the algorithm simulates the learning of the students (i.e., learners) through interaction among themselves. The students can also gain knowledge by discussing and interacting with other students. A learner will learn new information if the other learners have more knowledge than him or her. The learning phenomenon of this phase is expressed below:

```
for i=1: P_n
    Select any student randomly (Xj, i ≠j)
        if Xi is better than Xj
            Xnew=Xold + rand*(Xi-Xj)
        else
            Xnew=Xold + rand*(Xj-Xi)
        end
    if Xnew is better than Xold
Xi=Xnew
    end if
end for
```

The step-wise procedure for the implementation of TLBO is given as below:

Step 1 *generate initial population randomly*

Step 2 *calculate the mean of each design variable, i.e., mean(* X_i *)=* $\left(\sum_{j=1}^{P_n} X_{i,j}\right)/P_n$

Step 3 *define a student as a teacher whose objective function (f) is maximum*

Step 4 *update all student by using Eq. (13)*

Step 5 *compared students with each other (see computer code given in the section 3.1.2)*

Step 6 *is the termination criteria satisfied, if no, go to step 2.*

Step 7 *find the student whose objective function (f) is maximum and assign it as best solution*

In each phase, the objective function of the optimization problem is called by TLBO. So, the number of function evaluations are calculated two times more than the other algorithms such as GA and DE. The total number of function evaluation of the TLBO is calculated as $2*G_n*P_n+P_n+$, where "G_n" is the number of the iteration. However, the TLBO is an efficient algorithm to find global optimal solutions of the optimization problem.

3.2 Genetic algorithm (GA)

GA is a direct search algorithm based on the natural evolution concept coming from Darwin's theory of evolution. GA is a probability-based optimization algorithm which starts with an initial population of design variables. In GA, natural selection increases the surviving capability of the populations over the foregoing generations. The characteristics of each design are used to generate a fitness value indicating its level of performance with respect to the other designs in the population. Design variables that have the highest fitness value are given the greatest probability of breeding with other good designs so that their characteristics can be passed to the future generations. In this paper, optimization is carried out using the GA functions available in MATLAB using the GA toolbox. The most important GA operations which were used are: selection, crossover, and mutation and migration. Selection from the parent population is performed by the stochastic uniform function to make duplicates of better designs and eliminate the less valuable solutions. Crossover is implemented to recombine parent strings into child strings. For scattered crossover, a random binary vector was created. The genes of the child string were selected from the first parent where the binary vector component is 1 and from the second parent if it is 0. Crossover is usually applied with a high probability between 0.7 and 1.0 which in this study is chosen to occur with probability of 0.8. Mutation operator changes the parent vector string occasionally and is applied with a small probability, in order to prevent the GA from searching local minima. Gaussian mutation function is chosen for this purpose which adds a number to each component of the parent vector. This number is randomly chosen from a Gaussian distribution with mean 0. Forward migration is selected to specify how individuals move between subpopulations. In this way, migration (movement of individuals) occurs in the last subpopulation.

3.3 Differential evolution algorithm (DE)

The differential evolution (DE) algorithm firstly proposed by Storn and Price (1997) was proven to be one of the most promising global search methods and widely used to solve optimization problems in many fields such as communication, pattern recognition and mechanical engineering. The DE includes four main phases as follows:

3.3.1 Initialization

Initially, an initial population, includes NP individuals, is generated by means of randomly sampling from the search space. Each individual is a vector containing D_n design variables $X_i = (X_{i,1}, X_{i,2}, \ldots, X_{i,Dn})$ and is created by

$$X_{i,j} = X_j^l + \mathrm{rand}[0,1] * \left(X_j^u - X_j^1\right) \quad i = 1,2,\ldots P_n; \quad j = 1,2,\ldots,D_n \tag{18}$$

where X_j^l and X_j^u are the lower and upper bound of $X_{i,j}$, respectively, $\mathrm{rand}[0,1]$ is a uniformly distributed random number in [0,1].

3.3.2 Mutation

Secondly, each individual called the target vector X_i in the population is used to generate a mutant vector V_i via mutation operations. Some popular mutation operations are usually used in the DE as follows

$$-\mathrm{rand}/1 \quad V_i = X_{f_1} + F * \left(X_{f_2} - X_{f_3}\right) \tag{19}$$

$$-\mathrm{rand}/2 \quad V_i = X_{f_1} + F * \left(X_{f_2} - X_{f_3}\right) + F * \left(X_{f_4} - X_{f_5}\right) \tag{20}$$

$$-\mathrm{best}/1 \quad V_i = X_{best} + F * \left(X_{f_1} - X_{f_2}\right) \tag{21}$$

$$-\mathrm{best}/2 \quad V_i = X_{best} + F * \left(X_{f_1} - X_{f_2}\right) + F * \left(X_{f_3} - X_{f_4}\right) \tag{22}$$

-current-to-best/1:

$$V_i = X_i + F * (X_{best} - X_i) + F * \left(X_{f_1} - X_{f_2}\right) \tag{23}$$

where integers r_1, r_2, r_3, r_4, r_5 are randomly selected from $\{1,2,\ldots,P_n\}$ such that $r_1 \neq r_2 \neq r_3 \neq r_4 \neq r_5 \neq i$; the scale factor F is randomly chosen within [0,1], and X_{best}

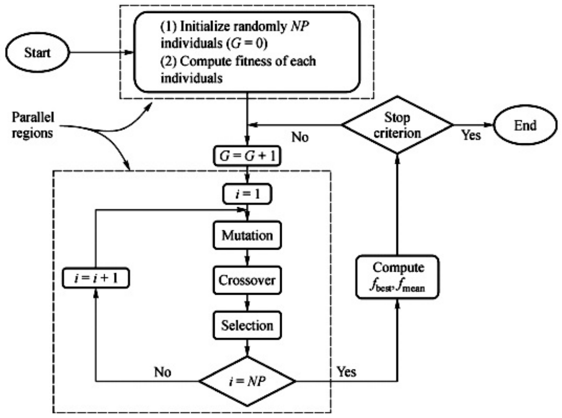

Fig. 2 A flow chart for implementation of differential evolution (DE) algorithm

is the best individual in the current population. After this phase, the jth components $V_{i,j}$ of mutant vector V_i are reflected back to allowable region if the boundary constraints are violated. This procedure is conducted as follows

$$V_{i,j} = \begin{cases} 2X_j^1 - V_{i,j} & \text{if } V_{i,j} < X_j^1 \\ 2X_j^u - V_{i,j} & \text{if } V_{i,j} > X_j^u \\ V_{i,j} & \text{otherwise} \end{cases} \quad (24)$$

3.3.3 Crossover

Thirdly, some elements of the target vector X_i are replaced by some elements of the mutant vector V_i to create a trial vector using binomial crossover operation

$$U_{i,j} = \begin{cases} V_{i,j} & \text{if rand}[0,1] \le CR \text{ or } j = j_{rand} \\ X_{i,j} & \text{otherwise} \end{cases} \quad (25)$$

where, $i \in \{1,2,\ldots,P_n\}, j \in \{1,2,\ldots,D_n\}$, j_{rand} is an integer selected from 1 to D_n and CR is the crossover control parameter.

3.3.4 Selection

Finally, based on the value of objective function, the trial vector U_i is compared to the target vector X_i. The better one having lower objective function value will survive to the next generation.

$$X_i = \begin{cases} U_i & \text{if } f(U_i) \le f(X_i) \\ X_i & \text{otherwise} \end{cases} \quad (26)$$

The flowchart of DE algorithm is summarized briefly in Fig. 2.

4. Optimization problem

Table 1 Uniaxial buckling load factors of a (0/90/0) laminate resting on the elastic foundation (b/h=10)

a/b	k_o	k_1	Akavci (2007)	Setoodeh and Karami (2004)	Xiang *et al.* (1996)	Present study
1	0	0	22.115	22.234	22.315	22.315
	100	0	32.247	32.235	32.447	32.447
	100	10	50.813	49.226	50.751	50.751
	0	0	16.308	16.424	16.434	16.434
2	100	0	32.247	32.254	32.447	32.447
	100	10	49.058	49.039	49.266	49.267

Table 2 Biaxial buckling load factors of a (0/90/0) laminate resting on the elastic foundation (b/h=10)

a/b	k_o	k_1	Akavci (2007)	Setoodeh and Karami (2004)	Xiang *et al.* (1996)	Present study
1	0	0	9.953	9.942	10.202	10.202
	100	0	11.980	11.923	12.228	12.229
	100	10	21.980	21.866	22.228	22.229
	0	0	3.261	3.269	3.286	3.287
2	100	0	9.350	9.345	9.590	9.590
	100	10	19.350	19.140	19.590	19.590

In this section, the optimal design problem for a laminated composite plate subjected to buckling load is formulated. The optimal design of laminated plates for maximum buckling load is more sophisticated than the other design parameters. The reason for the complexity is that buckling half-waves (n,m) that correspond to the critical buckling load are not known a priori and depend on the anisotropic properties such as lamination parameters and also design objectives. The design problem of a laminated plate with respect to the elastic instability can be stated as an optimization problem, where the objective is to find the optimum laminate lay-up that maximizes the critical buckling load. The mathematical formulation of the optimization problem is described as follows

$$\text{Maximize } \lambda_{cr}(\theta_i)$$
$$\text{Subject to } -90^o \le \theta_i \le 90^o, \qquad k=1, \ldots, N_L \quad (27)$$

where $\lambda_{cr}(\theta_i)$ is the critical buckling load, θ_i is the fibre orientation angle of the *i*th layer in which the fibre orientation angles are integer variables, N_L is the number of layers of the plate. The optimization procedure involves the stages of evaluating the critical buckling load for a given θ_i and improving the fibre orientations to maximize the critical buckling load λ_{cr}. Thus, the computational solution consists of succesive stages of analysis and optimization until a convergence is obtained and the optimal angle θ_{opt} is determined within a specified accuracy.

5. Numerical results and discussion

5.1 Comparison of the analytical solutions for the buckling analysis

Table 3 Statistical results of TLBO algorithm for 30 independent runs

Run no.	a/b	λ				θ_{opt} (°)			
		Best	Worst	Mean	Std				
1	1.0	34.5112	34.5015	34.5103	0.0020	44	-45	-45	45
	2.0	33.1152	32.2067	33.0089	0.2565	56	-55	-66	81
2	1.0	34.5112	34.4761	34.5066	0.0091	45	-46	-46	45
	2.0	33.1247	31.7799	33.0390	0.2586	56	-55	-68	82
3	1.0	34.5112	34.5106	34.5110	0.0002	45	-45	-45	44
	2.0	33.1257	33.0242	33.1085	0.0264	56	-55	-68	81
4	1.0	34.5112	34.4909	34.5098	0.0041	45	-46	-45	44
	2.0	33.1252	32.9791	33.1001	0.0361	-57	54	67	-80
5	1.0	34.5112	34.5111	34.5111	0.0000	45	-46	-45	44
	2.0	33.1255	32.0927	33.0644	0.1570	-57	54	67	-81
6	1.0	34.5112	34.5024	34.5100	0.0022	44	-45	-45	44
	2.0	33.1084	32.9328	33.0900	0.0253	56	-58	-58	78
7	1.0	34.5112	34.5053	34.5101	0.0016	44	-45	-45	44
	2.0	33.0916	32.7771	33.0305	0.0464	-57	51	73	83
8	1.0	34.5111	34.5037	34.5094	0.0024	44	-45	-45	44
	2.0	33.1255	32.5835	33.0944	0.0942	56	-55	-68	79
9	1.0	34.5112	34.4915	34.5067	0.0073	-45	44	44	-46
	2.0	33.1199	33.0297	33.1019	0.0228	-57	53	68	-86
10	1.0	34.5112	34.4976	34.5093	0.0039	45	-46	-45	44
	2.0	33.1168	32.5367	33.0691	0.0991	56	-55	-68	-90
11	1.0	34.5112	34.5071	34.5105	0.0011	-46	45	44	-45
	2.0	33.1211	32.9580	33.0767	0.0478	55	-56	-67	78
12	1.0	34.5112	34.5027	34.5099	0.0021	45	-45	-46	44
	2.0	33.1221	32.7183	33.0837	0.0782	56	-55	-68	83
13	1.0	34.5112	34.5066	34.5109	0.0007	44	-45	-45	44
	2.0	33.1042	33.0063	33.0668	0.0298	-56	59	54	-76
14	1.0	34.5112	34.4949	34.5087	0.0037	45	-45	-45	44
	2.0	33.1155	32.6949	33.0638	0.1099	56	-54	-70	-90
15	1.0	34.5112	34.0043	34.4960	0.0790	-46	45	44	-45
	2.0	33.1257	32.5259	33.0749	0.1132	-57	54	67	-80
16	1.0	34.5112	34.4935	34.5094	0.0044	-45	45	44	-45
	2.0	33.1257	32.8413	33.0942	0.0741	56	-55	-67	80
17	1.0	34.5112	34.4623	34.5080	0.0102	-46	44	45	-46
	2.0	33.1051	32.5781	33.0728	0.0756	55	-62	-51	75
18	1.0	34.5112	34.3502	34.4982	0.0400	-46	44	45	-45
	2.0	33.1259	31.3908	33.0710	0.2575	-57	54	67	-81
19	1.0	34.5112	34.4904	34.5083	0.0055	-45	44	44	-45
	2.0	33.1094	32.7998	33.0571	0.0646	-57	53	71	90
20	1.0	34.5112	34.4993	34.5102	0.0025	45	-46	-46	44
	2.0	33.1139	32.5280	33.0527	0.1101	56	-55	-68	-90
21	1.0	34.5112	34.3786	34.4886	0.0486	-46	45	45	-45
	2.0	33.1172	32.8347	33.0748	0.0744	-57	54	68	90
22	1.0	34.5112	34.3897	34.4419	0.0595	-45	44	45	-45
	2.0	33.1259	32.8151	33.0965	0.0665	56	-55	-68	80

23	1.0	34.5112	34.3909	34.4908	0.0427	-46	44	45	-46
	2.0	33.1246	32.5176	33.0651	0.1621	56	-54	-68	79
24	1.0	34.5112	34.2940	34.4924	0.0522	-46	44	45	-45
	2.0	33.1234	32.4804	33.0508	0.1467	-57	54	67	-80
25	1.0	34.5112	34.3644	34.4985	0.0385	-45	45	45	-46
	2.0	33.1250	32.4738	33.0638	0.1171	56	-55	-68	78
26	1.0	34.5112	34.4893	34.5097	0.0036	-46	44	45	-45
	2.0	33.1230	32.9729	33.1013	0.0288	-57	53	67	-80
27	1.0	34.5112	34.4789	34.5088	0.0055	-46	45	44	-45
	2.0	33.1225	32.8577	33.0900	0.0465	-57	53	67	-85
28	1.0	34.5112	34.5108	34.5111	0.0001	44	-45	-45	45
	2.0	33.1227	32.9254	33.0827	0.0510	-57	54	66	-78
29	1.0	34.5112	34.4772	34.5079	0.0081	-46	45	45	-46
	2.0	33.1207	32.8392	33.0565	0.0685	-57	54	68	-86
30	1.0	34.5112	34.4709	34.5069	0.0103	45	-45	-45	44
	2.0	33.1255	32.6017	33.0810	0.1296	56	-55	-68	79

In this section, the accuracy of the present analytical solutions for buckling analysis of simply supported cross-ply laminated composite plates (0/90/0) with or without elastic foundation under uniaxial and biaxial compression loads is examined (b/h=10). It is assumed that the thickness and the material properties for all lamina are the same. In the analysis, elastic lamina properties are assumed to be: $E_1/E_2 = 40$, $G_{12}/E_2 = G_{13}/E_2 = 0.6$, $G_{23}/E_2 = 0.5$, $\nu_{12} = 0.25$

The following relations are used for presentation of non-dimensional buckling load, non-dimensional linear Winkler foundation parameter and non-dimensional Pasternak foundation parameter, respectively

$$\lambda = \lambda_{cr}\frac{b^2}{E_2h^3}, \quad k_o = \frac{k_w b^4}{E_2h^3}, \quad k_o = \frac{k_s b^2}{E_2h^3} \qquad (28)$$

In Tables 1 and 2, the non-dimensional buckling load factors of simply supported cross-ply laminated composite plates (0/90/0) with or without elastic foundation are shown for uniaxial and biaxial loads, respectively.

As seen from Tables 1 and 2, the present results have suitable agreement with the literature results.

5.2 Optimization scheme

In the second section, the optimum stacking sequences of simply supported antisymmetric angle-ply laminates plates resting on Pasternak foundation subjected to compressive load are presented. Due to the absence of reference results in the literature related to the optimization problem, the optimum results obtained by the present method are compared with those solved by the Genetic Algorithm (GA) and Differential Evolution (DE) algorithms. In the optimization process, maximum number of iteration, number of population and total number of run are considered as 100, 50 and 30 for TLBO algorithm, respectively. In Table 3, the statistical results including best, worst, mean, standard deviation (Std) values of optimal buckling load factors are shown for 30 independent runs for the simply supported 8-layered antisymmetric angle-ply

Table 4 Optimum results for simply supported antisymmetric angle-ply square plates resting on Pasternak foundation subjected to uniaxial compressive load for different optimization algorithms ($k_o = 100$, $k_1 = 10$)

N	Methods	θ_{opt} (°)	λ
4	TLBO	$(14/-30)_{a,s}$	53.4198
	GA	$(-14/30)_{a,s}$	53.4198
	DE	$(-14/30)_{a,s}$	53.4198
8	TLBO	$(24/-24/-14/-1)_{a,s}$	54.6917
	GA	$(24/-24/-14/-1)_{a,s}$	54.6917
	DE	$(-24/24/14/1)_{a,s}$	54.6917
12	TLBO	$(-26/24/20/-13/-2/0)_{a,s}$	54.7083
	GA	$(-26/24/20/-13/-2/0)_{a,s}$	54.7083
	DE	$(26/-24/-20/13/2/0)_{a,s}$	54.7083

Table 5 Optimum results for simply supported antisymmetric angle-ply square plates resting on Pasternak foundation subjected to biaxial compressive load for different optimization algorithms ($k_o = 100$, $k_1 = 10$)

N	Methods	θ_{opt} (°)	λ
4	TLBO	$(-45/45)_{a,s}$	32.4645
	GA	$(-45/45)_{a,s}$	32.4645
	DE	$(45/-45)_{a,s}$	32.4645
8	TLBO	$(45/-45/-45/45)_{a,s}$	34.5112
	GA	$(-45/45/45/-45)_{a,s}$	34.5112
	DE	$(-45/45/45/-45)_{a,s}$	34.5112
12	TLBO	$(-45/45/-45/45/45/45)_{a,s}$	34.5112
	GA	$(45/-45/-45/45/45/-45)_{a,s}$	34.5112
	DE	$(-45/45/-45/45/45/45)_{a,s}$	34.5112

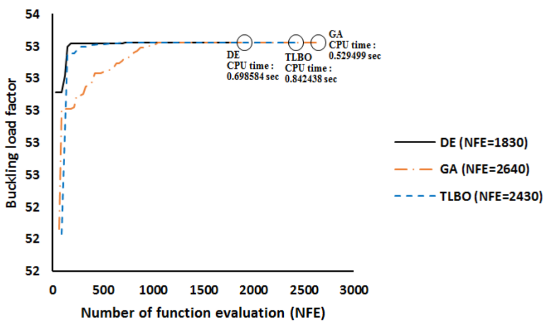

(a) 8 layers

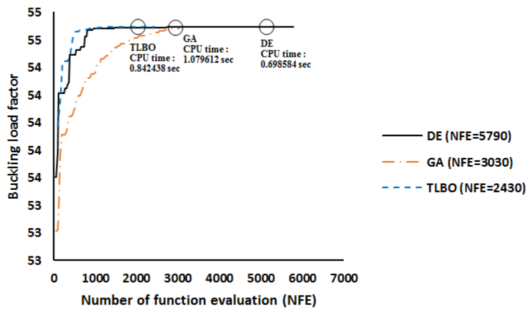

(b) 4 layers

Fig. 3 Convergence curves of buckling load factors for three different optimization algorithms

plates under biaxial load for different a/b ratios. (b/h=10, $k_o = 100$, $k_1 = 10$).

In Tables 4 and 5, the optimum results are given for simply supported antisymmetric angle-ply square plates resting on Pasternak foundation subjected to uniaxial and biaxial loads using three different algorithms for different number of layers (b/h=10, $k_o = 100$, $k_1 = 10$).

As seen from the Table 4 and Table 5, the optimum solutions obtained by TLBO agree very well with those solved by the GA and DE algorithms in terms of both fibre orientations and the critical buckling loads. It can be observed that the critical buckling loads are higher in the case of uniaxial loading compared to the biaxial loading. On the other hand, it can be seen from the results that as the number of layer increases, the critical buckling loads become almost the same. These results can be referred to the design engineers of composite plate-like structures. In Fig. 3, the convergence curves of buckling load factors for three different optimization algorithms are illustrated for simply supported antisymmetric angle-ply square plates resting on Pasternak foundation subjected to uniaxial load. (b/h=10, $k_o = 100$, $k_1 = 10$).

In Tables 6 and 7, effect of the plate aspect ratio on the optimum results is investigated for simply supported antisymmetric angle-ply plates resting on Pasternak foundation subjected to biaxial compressive load for different number of layers using three different algorithms (b/h=10, $k_o = 100$, $k_1 = 10$).

As seen from Tables 6 and 7, the critical buckling loads and optimum fibre orientations for TLBO algorithm are almost the same for those of the other two optimization

Table 6 Effect of the plate aspect ratio on the optimum results for simply supported 4-layered antisymmetric angle-ply plates resting on Pasternak foundation subjected to biaxial compressive load for different optimization algorithms (b/h=10, $k_o = 100$, $k_1 = 10$)

	TLBO		GA		DE	
a/b	θ_{opt} (°)	λ	θ_{opt} (°)	λ	θ_{opt} (°)	λ
1	$(-45/45)_{a,s}$	32.4645	$(45/-45)_{a,s}$	32.4645	$(45/-45)_{a,s}$	32.4645
1.5	$(57/-54)_{a,s}$	31.5020	$(57/-54)_{a,s}$	31.5019	$(-57/54)_{a,s}$	31.5020
2	$(57/-54)_{a,s}$	31.3926	$(-57/55)_{a,s}$	31.3919	$(57/-54)_{a,s}$	31.3926
2.5	$(58/-54)_{a,s}$	31.3400	$(58/-55)_{a,s}$	31.3391	$(-58/54)_{a,s}$	31.3400
3	$(58/-55)_{a,s}$	31.3101	$(-58/55)_{a,s}$	31.3101	$(58/-55)_{a,s}$	31.3101

Table 7 Effect of the plate aspect ratio on the optimum results for simply supported 8-layered antisymmetric angle-ply plates resting on Pasternak foundation subjected to biaxial compressive load for different optimization algorithms (b/h=10, $k_o = 100$, $k_1 = 10$)

	TLBO		GA		DE	
a/b	θ_{opt} (°)	λ	θ_{opt} (°)	λ	θ_{opt} (°)	λ
1	$(45/-45/-45/45)_{a,s}$	34.511222	$(-45/45/45/-45)_{a,s}$	34.5112	$(-45/45/45/-45)_{a,s}$	34.5112
1.5	$(-56/57/59/-71)_{a,s}$	33.2770	$(56/-57/-59/73)_{a,s}$	33.2768	$(56/-57/-59/71)_{a,s}$	33.2770
2	$(-57/54/67/-79)_{a,s}$	33.1259	$(-56/54/67/-81)_{a,s}$	33.1259	$(56/-54/-67/81)_{a,s}$	33.1260
2.5	$(57/-52/-74/-90)_{a,s}$	33.0539	$(57/-52/-74/90)_{a,s}$	33.0540	$(-57/52/74/-90)_{a,s}$	33.0542
3	$(57/-51/-79/-82)_{a,s}$	33.0301	$(57/-51/-80/-81)_{a,s}$	33.0299	$(-57/51/79/82)_{a,s}$	33.0306

Table 8 Effect of the nondimensional Winkler foundation stiffness (k_o) on the optimum results for simply supported 4-layered antisymmetric angle-ply square plates resting on Pasternak foundation subjected to biaxial compressive load for different optimization algorithms (b/h=10, $k_1 = 10$)

	TLBO		GA		DE	
k_o	θ_{opt} (°)	λ	θ_{opt} (°)	λ	θ_{opt} (°)	λ
0	$(45/-45)_{a,s}$	27.3985	$(-45/45)_{a,s}$	27.3985	$(45/-45)_{a,s}$	27.3985
20	$(-45/45)_{a,s}$	28.4117	$(45/-45)_{a,s}$	28.4117	$(45/-45)_{a,s}$	28.4117
40	$(-45/45)_{a,s}$	29.4249	$(-45/45)_{a,s}$	29.4249	$(-45/45)_{a,s}$	29.4249
60	$(-45/45)_{a,s}$	30.4381	$(-45/45)_{a,s}$	30.4381	$(45/-45)_{a,s}$	30.4381
80	$(-45/45)_{a,s}$	31.4513	$(45/-45)_{a,s}$	31.4513	$(-45/45)_{a,s}$	31.4513
100	$(45/-45)_{a,s}$	32.4645	$(45/-45)_{a,s}$	32.4645	$(45/-45)_{a,s}$	32.4645

algorithms. The non-dimensional buckling load decreases with increase in the plate aspect ratio and the effect of the aspect ratio on the buckling load is negligible for long plates. In Tables 8 and 9, the effect of nondimensional Winkler foundation stiffness (k_o) on the optimum results is investigated for simply supported antisymmetric angle-ply square plates resting on Pasternak foundation subjected to biaxial compressive load for different number of layers using three different algorithms (b/h=10, $k_1 = 10$). As seen, the critical buckling loads and optimum fibre

Table 9 Effect of the nondimensional Winkler foundation stiffness (k_o) on the optimum results for simply supported 8-layered antisymmetric angle-ply square plates resting on Pasternak foundation subjected to biaxial compressive load for different optimization algorithms (b/h=10, $k_1 = 10$)

	TLBO GA		GA		DE	
k_o	θ_{opt} (°)	λ	θ_{opt} (°)	λ	θ_{opt} (°)	λ
0	$(-45/45/45/-45)_{a,s}$	29.4451	$(45/-45/-45/45)_{a,s}$	29.4451	$(45/-45/-45/45)_{a,s}$	29.4451
20	$(-45/45/45/-45)_{a,s}$	30.4583	$(-45/45/45/-45)_{a,s}$	30.4583	$(-45/45/45/-45)_{a,s}$	30.4583
40	$(-45/45/45/-45)_{a,s}$	31.4715	$(-45/45/45/-45)_{a,s}$	31.4715	$(45/-45/-45/45)_{a,s}$	31.4715
60	$(-45/45/45/-45)_{a,s}$	32.4847	$(-45/45/45/-45)_{a,s}$	32.4847	$(45/-45/-45/45)_{a,s}$	32.4847
80	$(-45/45/45/-45)_{a,s}$	33.4980	$(45/-45/-45/45)_{a,s}$	33.4980	$(45/-45/-45/45)_{a,s}$	33.4980
100	$(-45/45/45/-45)_{a,s}$	34.5112	$(45/-45/-45/45)_{a,s}$	34.5112	$(45/-45/-45/45)_{a,s}$	34.5112

Table 10 Effect of the nondimensional shear stiffness (k_1) on the optimum results for simply supported 4-layered antisymmetric angle-ply square plates resting on Pasternak foundation subjected to biaxial compressive load for three different optimization algorithms (b/h=10, $k_o = 100$)

	TLBO		GA		DE	
k_1	θ_{opt} (°)	λ	θ_{opt} (°)	λ	θ_{opt} (°)	λ
0	$(-45/45)_{a,s}$	22.4645	$(-45/45)_{a,s}$	22.4645	$(45/-45)_{a,s}$	22.4645
2	$(-45/45)_{a,s}$	24.4645	$(-45/45)_{a,s}$	24.4645	$(45/-45)_{a,s}$	24.4645
4	$(45/-45)_{a,s}$	26.4645	$(-45/45)_{a,s}$	26.4645	$(-45/45)_{a,s}$	26.4645
6	$(45/-45)_{a,s}$	28.4645	$(-45/45)_{a,s}$	28.4645	$(-45/45)_{a,s}$	28.4645
8	$(-45/45)_{a,s}$	30.4645	$(45/-45)_{a,s}$	30.4645	$(-45/45)_{a,s}$	30.4645
10	$(45/-45)_{a,s}$	32.4645	$(-45/45)_{a,s}$	32.4645	$(-45/45)_{a,s}$	32.4645

Table 11 Effect of the nondimensional shear stiffness (k_1) on the optimum results for simply supported 8-layered antisymmetric angle-ply square plates resting on Pasternak foundation subjected to biaxial compressive load for three different optimization algorithms (b/h=10, $k_o = 100$)

	TLBO		GA		DE	
k_1	θ_{opt} (°)	λ	θ_{opt} (°)	λ	θ_{opt} (°)	λ
0	$(-45/45/45/-45)_{a,s}$	24.5112	$(-45/45/45/-45)_{a,s}$	24.5112	$(45/-45/-45/45)_{a,s}$	24.5112
2	$(45/-45/-45/45)_{a,s}$	26.5112	$(-45/45/45/-45)_{a,s}$	26.5112	$(-45/45/45/-45)_{a,s}$	26.5112
4	$(-45/45/45/-45)_{a,s}$	28.5112	$(45/-45/-45/45)_{a,s}$	28.5112	$(45/-45/-45/45)_{a,s}$	28.5112
6	$(-45/45/45/-45)_{a,s}$	30.5112	$(-45/45/45/-45)_{a,s}$	30.5112	$(45/-45/-45/45)_{a,s}$	30.5112
8	$(-45/45/45/-45)_{a,s}$	32.5112	$(-45/45/45/-45)_{a,s}$	32.5112	$(45/-45/-45/45)_{a,s}$	32.5112
10	$(-45/45/45/-45)_{a,s}$	34.5112	$(45/-45/-45/45)_{a,s}$	34.5112	$(-45/45/45/-45)_{a,s}$	34.5112

Table 12 Effect of load ratio (N_{yy}/N_{xx}) on the optimum results for simply supported 4-layered antisymmetric angle-ply square plates resting on Pasternak foundation subjected to biaxial compressive load for three different optimization algorithms (b/h=10, $k_o = 100$, $k_1 = 10$)

	TLBO GA		GA		DE	
N_{yy}/N_{xx}	θ_{opt} (°) (°)	λ	θ_{opt} (°) (°)	λ	θ_{opt} (°) (°)	λ
1/4	$(27/-33)_{a,s}$	49.1358	$(-27/-33)_{a,s}$	49.1357	$(27/-33)_{a,s}$	49.1358
1/2	$(40/-40)_{a,s}$	43.0579	$(-40/40)_{a,s}$	43.0576	$(40/-40)_{a,s}$	43.0579
1	$(-45/45)_{a,s}$	32.4645	$(45/-45)_{a,s}$	32.4645	$(45/-45)_{a,s}$	32.4645
2	$(50/-50)_{a,s}$	21.5289	$(50/-50)_{a,s}$	21.5289	$(50/-50)_{a,s}$	21.5289
4	$(63/-57)_{a,s}$	12.2839	$(63/-56)_{a,s}$	12.2839	$(-63/57)_{a,s}$	12.2839

Table 13 Effect of load ratio (N_{yy}/N_{xx}) on the optimum results for simply supported 8-layered antisymmetric angle-ply square plates resting on Pasternak foundation subjected to biaxial compressive load for three different optimization algorithms (b/h=10, $k_o = 100$, $k_1 = 10$)

	TLBO		GA		DE	
N_{yy}/N_{xx}	θ_{opt} (°) (°)	λ	θ_{opt} (°) (°)	λ	θ_{opt} (°) (°)	λ
1/4	$(28/-28/-18/2)_{a,s}$	51.2996	$(-28/28/17/-1)_{a,s}$	51.2995	$(-29/28/18/-1)_{a,s}$	51.2996
1/2	$(-40/39/38/-27)_{a,s}$	45.6514	$(40/-39/-38/27)_{a,s}$	45.6513	$(-40/39/38/-28)_{a,s}$	45.6515
1	$(-45/45/45/-45)_{a,s}$	34.5112	$(-45/45/45/-45)_{a,s}$	34.5112	$(-45/45/45/-45)_{a,s}$	34.5112
2	$(50/-51/-53/62)_{a,s}$	22.8256	$(50/-51/-52/65)_{a,s}$	22.8253	$(50/-51/-52/62)_{a,s}$	22.8257
4	$(-62/62/73/90)_{a,s}$	12.8247	$(-62/61/74/-90)_{a,s}$	12.8247	$(-62/62/72/-89)_{a,s}$	12.8249

orientations for TLBO algorithm are the same for those of GA and DE algorithms. On the other hand, as the Winkler foundation stiffness increases, the critical buckling load increases. However, there is no any effect of the Winkler foundation stiffness on the optimum fibre orientations.

In Tables 10 and 11, the effect of the nondimensional shear stiffness (k_1) on the optimum results is investigated for simply supported antisymmetric angle-ply square plates resting on Pasternak foundation subjected to biaxial compressive load for different number of layers using three different optimization algorithms (b/h=10, $k_o = 100$). As seen, the critical buckling loads and optimum fibre orientations for TLBO algorithm are the same for those of GA and DE algorithms. On the other hand, as the shear stiffness increases, the critical buckling load increases. However, there is no any effect of the shear stiffness on the optimum fibre orientations.

In Tables 12 and 13, the effect of load ratio (N_{yy} / N_{xx}) on the optimum results is investigated for simply supported antisymmetric angle-ply square plates resting on Pasternak foundation subjected to biaxial compressive load for different number of layers using three different optimization algorithms (b/h=10, $k_o = 100$, $k_1 = 10$). As seen from Table 12 and Table 13, the critical buckling loads and optimum fibre orientations for TLBO algorithm are almost the same for those of the other two optimization algorithms. On the other hand, as the load ratio increases, the critical buckling load decreases. However, the load ratio has a substantial effect on the optimum fibre orientations.

6. Conclusions

This paper deals with the maximization of the critical buckling load of simply supported antisymmetric angle-ply plates resting on Pasternak foundation subjected to compressive loads using teaching learning based optimization method (TLBO). The first order shear deformation theory is used to obtain governing equations of the laminated plate. In the present optimization problem, the objective function is to maximize the buckling load factor and the design variables are the fibre orientation angles in the layers. Computer programming is developed in the MATLAB environment to estimate optimum stacking sequences of laminated plates. Finally, the influences of different number of layers, plate aspect ratios, foundation parameters and load ratios on the optimal solutions are investigated. As seen from the results that, the optimum results for TLBO algorithm are almost the same for the results of GA and DE algorithms for all parameters. The critical buckling loads are higher in the case of uniaxial loading compared to the biaxial loading. As the number of layer increases, the critical buckling loads become almost the same. The non-dimensional buckling load decreases with increase in the plate aspect ratio and the effect of the aspect ratio on the buckling load is negligible for long plates. As the foundation parameters increase, the critical buckling loads increase. However, there is no any effect of the foundation parameters on the optimum fibre orientations. As the load ratio increases, the critical buckling load decreases. However, the load ratio has a substantial effect on the optimum fibre orientations. The obtained results of the optimization problems show that TLBO is suitable and effective algorithm for solving the critical buckling load optimization problems of laminated composite plates resting on Pasternak foundation.

References

Adali, S., Lene, F., Duvaut, G. and Chiaruttini, V. (2003), "Optimization of laminated composites subject to uncertain buckling loads", *Compos. Struct.*, **62**, 261-269.

Akavci, S.S. (2007), "Buckling and free vibration analysis of symmetric and antisymmetric laminated composite plates on an elastic foundation", *J. Reinf. Plast. Compos.*, **26**, 1907-1919.

Artar, M. (2016), "Optimum design of braced steel frames via teaching learning-based optimization", *Steel Compos. Struct.*, **22**, 733-744.

Artar, M., Catar, R. and Daloglu, A.T. (2017), "Optimum design of steel bridges including corrosion effect using TLBO", *Struct. Eng. Mech.*, **63**, 607-615.

Aymerich, F. and Serra, M. (2008), "Optimization of laminate stacking sequence for maximum buckling load using the ant colony optimization (ACO) metaheuristic", *Compos. Part A*, **39**, 262-272.

Daloglu, A.T., Artar, M., Ozgan, K. and Karakas, A.I. (2018), "Optimum design of braced steel space frames including soil-structure interaction via Teaching-learning-based optimization and Harmony search algorithms", *Adv. Civil Eng.*

De Almeida, F.S. (2016), "Stacking sequence optimization for maximum buckling load of composite plates using harmony search algorithm", *Compos. Struct.*, **143**, 287-299.

Deveci, H.A., Aydin, L. and Artem, H.S. (2016), "Buckling optimization of composite laminates using a hybrid algorithm under Puck failure criterion constraint", *J. Reinf. Plast. Compos.*, **35**, 1233-1247.

Ehsani, A. and Rezaeepazhand, J. (2016), "Stacking sequence optimization of laminated composite grid plates for maximum buckling load using genetic algorithm", *Int. J. Mech. Sci.*, **119**, 97-106.

Erdal, O. and Sonmez, F.O. (2005), "Optimum design of composite laminates for maximum buckling load capacity using simulated annealing", *Compos. Struct.*, **71**, 45-52.

Hajmohammad, M.H., Salari, M., Hashemi, S.A. and Esfe, M.H. (2013), "Optimization of stacking sequence of composite laminates for optimizing buckling load by neural network and genetic algorithm", *Ind. J. Sci. Technol.*, **6**, 5070-5077.

Henrichsen, S.R., Lindgaard, E. and Lund, E. (2015), "Robust buckling optimization of laminated composite structures using discrete material optimization considering "worst" shape imperfections", *Thin Walled Struct.*, **94**, 624-635.

Huu, V.H., Thi, T.D.D., Trung, H.D., Duy, T.V. and Thoi, T.N. (2016), "Optimization of laminated composite plates for maximizing buckling load using improved differential evolution and smoothed finite element method", *Compos. Struct.*, **146**, 132-147.

Jing, Z., Fan, X. and Sun, Q. (2015), "Stacking sequence optimization of composite laminates for maximum buckling load using permutation search algorithm", *Compos. Struct.*, **121**, 225-236.

Karakaya, S. and Soykasap, O. (2009), "Buckling optimization of laminated composite plates using genetic algorithm and generalized pattern search algorithm", *Struct. Multidisc. Optim.*, **39**, 477-486.

Kaveh, A. (2017), *Advances in Metaheuristic Algorithms for Optimal Design of Structures*, 2nd Edition, Springer International Publishing, Switzerland.

Kaveh, A. and Farhoudi, N. (2013), "A new optimization method: Dolphin echolocation", *Adv. Eng. Softw.*, **59**, 53-70.

Kaveh, A. and Ghazaan, M.I. (2017), "Vibrating particles system algorithm for truss optimization with multiple natural frequency constraints", *Acta Mech.*, **228**, 307-322.

Kaveh, A. and Khayatazad, M. (2012), "A new meta-heuristic method: Ray optimization", *Compos. Struct.*, **112-113**, 283-294.

Kaveh, A. and Mahdavi, V.R. (2014), "Colliding bodies optimization: A novel meta-heuristic method", *Compos. Struct.*, **139**, 18-27.

Kaveh, A., Dadras, A. and Malek, N.G. (2018), "Buckling load of laminated composite plates using three variants of the biogeography-based optimization algorithm", *Acta Mech.*, **229**, 1551-1566.

Moez, H., Kaveh, A. and Taghizdieh, N. (2016), "Natural forest regeneration algorithm: A new meta-heuristic", *Iran. J. Sci. Technol.*, **40**, 311-326.

Narita, Y. and Turvey, G.J. (2004), "Maximizing the buckling loads of symmetrically laminated composite rectangular plates using a layerwise optimization approach", *Proc. Inst. Mech. Eng. Part C J. Mech. Eng. Sci.*, **218**, 681-691.

Nicholas, P.E., Padmanaban, K.P. and Vasudevan, D. (2014), "Buckling optimization of laminated composite plate with elliptical cutout using ANN and GA", *Struct. Eng. Mech.*, **52**, 815-827.

Rao, R.V., Savsani, V.J. and Vakharia, D.P. (2011), "Teaching-learning-based optimization: A novel method for constrained mechanical design optimization problems", *Comput. Des.*, **43**, 303–315.

Reddy, J.N. (2004), *Mechanics of Laminated Composite Plates and Shells-Theory and Analysis*, 2nd Edition, CRC Press.

Sebaey, T.A., Lopes, C.S., Blanco, N. and Costa, J. (2011), "Ant colony optimization for dispersed laminated composite panels under biaxial loading", *Compos. Struct.*, **94**, 31-36.

Setoodeh, A.R. and Karami, G. (2004), "Static, free vibration and buckling analysis of anisotropic thick laminated composite plates on distributed and point elastic supports using a 3-D layer-wise FEM", *Eng. Struct.*, **26**, 211-220.

Soremekun, G., Gürdal, Z., Haftka, R.T. and Watson, L.D. (2011), "Composite laminate design optimization by genetic algorithm with generalized elitist selection", *Comput. Struct.*, **79**, 131-143.

Storn, R. and Price, K. (1997), "Differentiale evolution-a simple and efficient heuristic for global optimization over continuous spaces", *J. Glob. Optim.*, **11**, 341-359.

Topal, U. (2017), "Buckling load optimization of laminated composite stepped columns", *Struct. Eng. Mech.*, **62**, 107-111.

Topal, U. and Ozturk, H.T. (2014), "Buckling load optimization of laminated plates via artificial bee colony algorithm", *Struct. Eng. Mech.*, **52**, 755-765.

Vosoughi, A.R., Darabi, A. Forkhorji, H.D. (2017), "Optimum stacking sequences of thick laminated composite plates for maximizing buckling load using FE-GAs-PSO", *Compos. Struct.*, **159**, 361-367.

Vosoughi, A.R., Darabi, A., Anjabin, N. and Topal, U. (2017), "A mixed finite element and improved genetic algorithm method for maximizing buckling load of stiffened laminated composite plates", *Aerosp. Sci. Technol.*, **70**, 378-387.

Xiang, Y., Kitipornchai, S. and Liew, K.M. (1996), "Buckling and vibration of thick laminates on Pasternak foundations", *J. Eng. Mech.*, **122**, 54-63.

CC